Supplemental Material for

Thomas, R. Q., E. Brooks, A. Jersild, E. Ward, R. Wynne, T.J. Albaugh, H. D. Aldridge, H. E. Burkhart, J-C Domec, T. R. Fox, C. A. Gonzalez-Benecke, T. A. Martin, A. Noormets, D. A. Sampson, and R. O. Teskey. Leveraging 35 years of forest research in the southeastern U.S. to constrain carbon cycle predictions: regional data assimilation using ecosystem experiments.

Description of 3-PG model

Our analysis used a modified version of the 3-PG model. For completeness, we describe the entire model and highlight our modifications.

Monthly carbon assimilation (gross primary productivity; GPP) was based on absorbed photosynthetically active radiation (APAR) and a quantum yield variable (α_e) described below in Equation 5 (Bryars et al., 2013; Gonzalez-Benecke et al., 2016; Landsberg and Waring, 1997).

$$\mathrm{GPP}=\mathrm{APAR}\times\alpha_e \qquad \text{Equation 1}$$

APAR was a function of the down-welling photosynthetically active radiation (PAR), the leaf area index (LAI), and the canopy closure.

$$\mathrm{APAR}=\mathrm{PAR}\times(1-e^{(-k\times \mathrm{LAI})})\times f(\mathrm{closure}) \qquad \text{Equation 2}$$

The canopy closure function, f(closure), increased APAR as a stand reached a parameterized age of canopy closure (fullCanAge) (Bryars et al., 2013).

$$f(\mathrm{closure})=\min\left(1,\frac{\mathrm{StandAge}}{\mathrm{fullCanAge}}\right) \qquad \text{Equation 3}$$

StandAge was a variable describing the age of the simulated stand. LAI was a derived variable calculated by dividing the foliage biomass (WF) by a specific leaf area (SLA). Based on (Gonzalez-Benecke et al., 2016), SLA decreased as a stand aged.

$$\mathrm{SLA}=\mathrm{SLA1}+(\mathrm{SLA0}-\mathrm{SLA1})\times e^{\left(-\ln(2)\times\left(\frac{\mathrm{StandAge}}{\mathrm{tSLA}}\right)^2\right)} \qquad \text{Equation 4}$$

The variable α_e was a function of a maximum quantum yield parameter (α) modified by mean daily air temperature (T_{avg}), number of frost days (FrostDays), available soil water (ASW), vapor pressure deficit (VPD), atmospheric CO_2 concentration, stand age, and soil fertility (FR) where each of the modifiers took a value between 0 and 1 (except for the CO_2 modifier which took values greater than 1 if atmospheric CO_2 was greater than 350 ppm).

$$\alpha_e= \alpha\times f(T_{avg})\times f(\mathrm{FrostDays},T_{min})\times f(\mathrm{VPD})\times f(\mathrm{ASW})\times f(CO_2)\times f(\mathrm{Age})\times \mathrm{FR} \qquad \text{Equation 5}$$

The mean daily temperature modifier, $f(T_{avg})$, was based on a parameterized optimum (T_{opt}), maximum (T_{max}), and minimum (T_{min}) temperature of photosynthesis using

$$f(T_{avg})=\frac{(T_{avg}\text{-}T_{min})}{(T_{avg}\text{-}T_{min})}\times\frac{(T_{max}\text{-}T_{avg})}{(T_{max}\text{-}T_{opt})}^{\frac{(T_{max}\text{-}T_{opt})}{(T_{opt}\text{-}T_{min})}} \qquad \text{Equation 6}$$

The frost day modifier, f(FrostDays, T_{min}^{met}), decreased carbon assimilation proportional to the number of days during the month with minimum temperature below -1°C (FrostDays) (Bryars et al., 2013).

$$f(\text{frostday},T_{min})=1\text{-}\left[\left(1\text{-}e^{kF*T_{min}^{met}}\right)\times\frac{\text{FrostDays}}{30}\right] \qquad \text{Equation 7}$$

The magnitude of the decrease was an exponential function of the mean daily minimum temperature over the month, T_{min}^{met} (Gonzalez-Benecke et al., 2016). The vapor pressure deficit modifier, f(VPD), was an exponential function where the modifier decreased as mean daily VPD increased (Gonzalez-Benecke et al., 2016).

$$f(\text{VPD})=e^{\text{-CoeffCond}\times\text{VPD}} \qquad \text{Equation 8}$$

The soil moisture modifier, f(ASW), was a logistic function of the ASW relative to a specified maximum available soil water (MaxASW) (Landsberg and Waring, 1997).

$$f(\text{ASW})=\frac{1}{1+\left[\frac{(1-moist\_ratio)}{SWconst}\right]^{\text{SWpower}}} \qquad \text{Equation 9}$$

where

$$\text{moist\_ratio}=\frac{\text{ASW}}{\text{MaxASW}} \qquad \text{Equation 10}$$

In this version, the two parameters governing the soil moisture modifier function were the same across all soil types. Therefore, MaxASW was the key difference between sites. The soil texture dependent parameters used in prior applications of 3-PG were removed to simplify the number of parameters in the model and could be reintroduced and optimized in future applications.

The atmospheric CO_2 modifier, f(CO_2), was a saturating function of atmospheric CO_2, where the modifier was set to one at 350 ppm (Almeida et al., 2009). The atmospheric CO_2 modifier was able to have values greater than one when atmospheric CO_2 was greater than 350 ppm.

$$f(CO_2)=\frac{\text{fCalpha}_x\times CO_2}{350\times(\text{fCalpha}_x\text{-}1)+CO_2} \qquad \text{Equation 11}$$

where

$$\text{fCalpha}_x=\frac{\text{fCalpha700}}{(2\text{-fCalpha700})} \qquad \text{Equation 12}$$

The age modifier, f(Age), decreased canopy quantum yield as a stand aged (Bryars et al., 2013).

$$f(Age)=\frac{1}{1+\left[\frac{RelAge}{rAge}\right]^{nAge}}$$ Equation 13

where

$$RelAge=\frac{StandAge}{MaxAge}$$ Equation 14

MaxAge did not represent the maximum possible age of a stand, rather it was a parameter controlling the shape of Equation 13. It is possible for MaxAge and nAge to be parameterized so that the age modifier was effectively one for all ages (i.e., no decline in quantum yield as a stand ages). Therefore, the calibrated value of MaxAge could be older than the age of a typical harvest rotation

The soil fertility modifier, FR, was a proxy for the nutrient availability. In prior applications of the 3-PG model, FR was a site-specific value between zero and one (Bryars et al., 2013; Landsberg and Waring, 1997) that modified the quantum use efficiency and the allocation to total roots (prior applications of 3-PG combined fine and coarse roots). To simplify parameters and assumptions in the 3-PG model for application to data assimilation, we modified 3-PG so that FR only modified quantum use efficiency. Therefore, for a given LAI and climatic conditions, a lower FR represented a reduced capacity to convert light captured by LAI to photosynthate. In turn, lower photosynthesis at the site with lower FR will lead to lower LAI. An FR of one indicated that the site was not limited by nutrient availability. FR values less than one represented the degree of nutrient limitation at the site.

FR could be estimated for a site or could be estimated from biophysical covariates. In the former, FR is directly estimated for a site, which effectively represents a fixed effect in a statistical model. However, fixing FR for each site used in optimization does not allow for predictions at sites that were not used in calibration because FR at a new site would be unknown. Alternatively, FR could be a function of site characteristics that allow for spatial predictions of FR based on maps of the characteristics. We used a hybrid of these two approaches.

First, we used site index (SI; the mean height of dominant or co-dominant trees for a specified base age: 25 years, in this study) and mean annual temperature (MAT) to predict FR at sites that did not receive nutrient additions. Site index has previously been used to predict FR using a saturating or logistic function (Gonzalez-Benecke et al., 2016; 2014b; Subedi et al., 2015). Site index is a useful metric of stand productivity because it is commonly measured or modeled (Sabatia and Burkhart, 2014) and integrates many environmental factors that influence growth. When comparing sites with similar climate and available soil water, site index represents differences in nutrient bioavailability. Since site index integrates multiple environmental factors beyond nutrient bioavailability, including factors that are already represented in the prediction of photosynthesis (climate, available soil water, etc.), the influence of these other environmental factors should be factored out of the relationship between site index and FR. This helps avoids covariance between FR parameterization and the parameterization of other environmental modifiers and avoids double counting the influence of the other environmental factors on photosynthesis. We used the long-term MAT for the site to represent the environmental factors that are already accounted for in the photosynthesis calculating and modified the saturating function of the site SI in (Gonzalez-Benecke et al., 2014b; 2016) to include a temperature modifier,

$$FR=\frac{1}{1+e^{FR1\times MAT\ -\ FR2\times SI}} \qquad \text{Equation 15}$$

Equation 15 assumed that same SI should correspond to a lower FR in stands at the warmer extent of the species range (i.e., Southern Georgia) than stands in the cooler extent (i.e., Virginia) (Figure 1a). FR1 and FR2 are the parameters governing the shape of the relationship. The MAT used in Equation 15 was based on the 35-year mean annual temperature of site (1979-2011; (Abatzoglou, 2013)) and did not vary during a simulation. By not varying during a simulation and averaging over a 35-year period, MAT represented a long-term climatic driver of soil fertility rather than an inter- and intra-annual driver of fertility.

Second, we directly estimated FR for sites that received nutrient additions and for the sites simulated in the first stage of data assimilation (see main text for a description of the first and second stage of data assimilation). For nutrient addition sites, we treated FR as an estimated site-specific parameter that must be equal to or greater than the FR predicted by equation 15 for the corresponding control plot. A previous application of the 3-PG model to the loblolly pine ecosystem used a parameter to control the sensitivity of quantum yield to FR, parameter FN_0(Bryars et al., 2013). Here, we set FN_0 equal to zero to prevent covariation and identifiability issues with the FR parameters in Equation 15.

A fixed fraction (y) of GPP (equation 1) was available for growth as net primary production (NPP), which assumed a time and space invariant NPP to GPP ratio (Bryars et al., 2013; Gonzalez-Benecke et al., 2016).

$$NPP=GPP\times y \qquad \text{Equation 16}$$

NPP was allocated to leaf biomass (pF), stem (bole + branches) biomass (pWS), coarse root biomass (pWCR), and fine root biomass (pFR). The pattern of NPP allocation to plant tissues varied as the average size of the average tree increased. Specifically, the ratio of NPP allocated to leaf biomass versus stem biomass (pFS) asymptotically decreased as the average diameter of a tree at the site increased (Bryars et al., 2013).

$$pFS=\left(pfsConst\times avDBH^{pfsPower}\right)\times fCpFS \qquad \text{Equation 17}$$

where pfsPower and pfsConst were functions of foliage to stem allocation at 2 cm (pFS20) and 20 cm diameter (pFS2)

$$pfsPower=\frac{\log\left(\frac{pFS20}{pFS2}\right)}{\log\left(\frac{20}{2}\right)} \qquad \text{Equation 18}$$

$$pfsCont=\frac{pFS2}{2^{pfspower}} \qquad \text{Equation 19}$$

The average diameter of a tree (avDBH) used in the allocation calculation was based on an allometric relationship between biomass of the average tree (AvStemMass) and diameter (Gonzalez-Benecke et al., 2014a).

$$avDBH=\left(\frac{AvStemMass}{stemConst}\right)^{\frac{1}{stemPower}} \qquad \text{Equation 20}$$

AvStemMass assumed that all trees had equal stem biomass (WS) by dividing WS by the number of stems (ha^{-1}) in the stand (StemNumber)

$$AvStemMass=\frac{WS}{StemNumber} \qquad \text{Equation 21}$$

In our version of 3-PG, the ratio of leaf to stem biomass also decreased with atmospheric CO_2 based on the following

$$fCpFS=\frac{fCpFS_x \times CO_2}{350\times(2fCpFS_x\text{-}1)+CO_2} \qquad \text{Equation 22}$$

where

$$fCpFS_x=\frac{fCpFS700}{(2\text{-}fCpFS700)} \qquad \text{Equation 23}$$

In our modified version, we separated coarse roots and fine roots. Coarse root biomass was parameterized as a constant fraction of stem biomass allocation (pCRS) and fine root biomass was parameterized as constant proportion of foliage allocation (pRF). Due to the limited availability of fine root biomass data, we removed the dependence of total root allocation (fine and coarse roots) on nutrient, soil water, and vapor pressure deficit that was used in previous versions of the 3-PG (Bryars et al., 2013; Gonzalez-Benecke et al., 2016).

We introduced a two-cohort model to simulate the turnover of leaf biomass (variable: leaf_turnover). The life span of loblolly pine needles has been shown to be approximately two years (Albaugh et al., 2010; Sampson et al., 2003). The turnover of leaf biomass was assumed to occur in November and to represent 100% of the second-year cohort biomass. Allocation to leaf biomass was always to a first-year cohort. Cohort 1 transferred to cohort 2 at the end of the calendar year. Therefore, the three parameters associated with leaf turnover used in previous versions of the 3-PG model were removed from our version. In contrast to leaf dynamics, fine roots were a single cohort and the turnover was a constant proportion throughout the year (root_turnover).

$$root\_turnover= Rttover\times WR \qquad \text{Equation 24}$$

The turnover of stem and coarse roots was based on a density-dependent mortality rate and constant density-independent mortality rate. The density-dependent mortality rate used a self-thinning law to decrease the number of stems as the average size of a tree increases. Following (Landsberg and Waring, 1997), the stem count (StemNumber) was reduced (stem_turnover_depend) if the average individual tree stem biomass (AvStemMass) was above the thinning curve (the relationship between average stem biomass and total stems per hectare) . The thinning curve was parameterized by the maximum average stem mass using the WS_{x1000} and ThinPower parameters

$$WS_{max}=WS_{x1000}\times AvStemMass^{ThinPower} \quad \text{Equation 25}$$

Details of how the self-thinning processes was solved can be found in Landsberg and Waring (1997). The stem biomass turnover that was associated with the density-dependent mortality was calculated by assuming that trees that died from thinning were smaller (ms) than the average sized tree in the stand

$$ws\_turnover\_depend = ms\times \frac{WS}{StemNumber}\times stem\_turnover\_depend \quad \text{Equation 26}$$

where ms was the parameter governing the proportion of an averaged size tree that died during self-thinning. Similarly, coarse roots (WCR) died through the same self-thinning process.

$$wcr\_turnover\_depend = ms\times \frac{WCR}{StemNumber}\times stem\_turnover\_depend \quad \text{Equation 27}$$

In our modified version, we added a density-independent mortality rate that was a constant fraction (mort_rate) of stems and coarse roots

$$ws\_turnover\_independ = ms\times WS\times mort\_rate \quad \text{Equation 28}$$

$$wcr\_turnover\_independ = ms\times WCR\times mort\_rate \quad \text{Equation 29}$$

No foliage or fine roots were removed when a tree died through density-independent mortality because their turnover was already accounted for in the leaf-life span calculation and the fine root turnover parameter. Therefore, the parameters mF and mR used in previous applications of the 3-PG model were set to zero.

Evapotranspiration (ET) was the sum of canopy transpiration and evaporated fraction of rain intercepted by the canopy. The calculation of canopy transpiration used a Penman-Monteith approach that depended on canopy conductance (Conductance), boundary layer conductance (BLcond), vapor pressure deficit, and net radiation (Landsberg and Waring, 1997). Transpiration was further modified by the number of frost days according to the frost day function, f(FrostDays), described in Equation 7. Conductance increased to a maximum canopy conductance (MaxCond) as LAI increased to a value equal or greater than the LAI of maximum conductance (LAIgcx**)**. Cond was influenced by VPD, ASW, and stand age using the same modifiers as used in the photosynthesis calculation (Equation 5).

$$Conductance=MaxCond \times \min[1, \left(\frac{LAI}{LAI_{gcx}}\right)]\times fg(CO2) \times f(VPD) \times f(ASW)\times f(Age)$$

Equation 30

The CO_2 modifier, $fg(CO_2)$ allowed for Cond to decline as atmospheric CO_2 increased based on a parameterized reduction in canopy conductance between 350 and 700 ppm atmospheric CO2 concentration (fCg700)

$$fg(CO_2)= \frac{fCg_0}{1+(fCg_0-1)\times\left(\frac{CO_2}{350}\right)} \quad \text{Equation 31}$$

where

$$fCg_0=\frac{fCg700}{(2\times fCpFS700-1)} \quad \text{Equation 32}$$

In our application to loblolly pines, we assumed that stomatal conductance did not decrease as atmospheric CO_2 levels increased because sap flux measurements at the Duke FACE study found that stomatal conductance on a ground area basis did not change with elevated CO_2 (Ward et al., 2013). The maximum conductance parameter (MaxCond) was shared across all sites.

Intercepted rain was assumed to return to the atmosphere through evaporation. Intercepted rain increased with LAI to a maximum (MaxIntcptn) at a parameterized LAI value (LAImaxIntcptn)

$$Interception= Rain\times MaxIntcptn \times \min\left(1.0, \frac{LAI}{LAImaxIntcptn}\right) \quad \text{Equation 33}$$

Runoff occurred when soil water exceeded the specified site-level maximum available soil water after accounting for rain and evapotranspiration during the month.

To facilitate the most robust integration of eddy-covariance estimates of gross ecosystem productivity (GPP estimated using eddy-covariance measurements) and ET from stands with hardwood species in the understory, we added the capacity to simulate understory hardwoods. The calculation of hardwood photosynthesis parallels the calculation for the overstory pines except that: 1) the PAR available to the understory was the transmitted PAR after pine absorbance, 2) a separate GPP was calculated using the transmitted PAR and an understory specific maximum quantum yield (α_h), 2) the allocation parameters were specific to the understory (pFS_h, pRF_h and pCRS_h), 4) only density-independent mortality (mort_rate_h) was simulated, 5) NPP was added to a bud biomass pool, and 6) spring growth of foliage was from the bud biomass pool (Bud_to_leaf). The temperature, VPD, frost day, soil fertility, and soil water modifiers were equal to those used for the overstory pines. LAI was calculated for the understory hardwoods by dividing the foliage biomass (WFh) by the hardwood specific leaf area (SLAh). Unlike the overstory pines, SLAh was a parameter and did not vary with stand age. The LAI value used in the canopy conductance calculation was the sum of pine and hardwood LAI and the maximum conductance parameter (MaxCond) was assumed to apply to both pine and hardwood trees. Canopy transpiration was assigned to pine and hardwoods based on the proportion of total LAI. The hardwood understory dropped leaves in November and growth leaves in April. Therefore, the simulated photosynthesis and ET during the winter months was solely from the pines in the stand.

Overall, the 3-PG model used in this study simulated the monthly change in eleven state variables per plot: four stocks for pines, five stocks for understory hardwoods, pine stem density (stems ha^{-1}), and available soil water (ASW).

$$\frac{dWF}{dt} = NPP \times pF - leaf\_turnover \qquad \text{Equation 34}$$

$$\frac{dWS}{dt} = NPP \times pS - ws\_turnover\_depend - ws\_turnover\_independ \qquad \text{Equation 35}$$

$$\frac{dWCR}{dt} = NPP \times pCR - wcr\_turnover\_depend - wcr\_turnover\_independ \qquad \text{Equation 36}$$

$$\frac{dWR}{dt} = NPP \times pR - root\_turnover - wr\_turnover\_depend \qquad \text{Equation 37}$$

$$\frac{dStemNumber}{dt} = -StemNumber \times mort\_rate - stem\_turnover\_depend \qquad \text{Equation 38}$$

$$\frac{dASW}{dt} = rain + irrigation - canopy\_transpiration - interception \qquad \text{Equation 39}$$

where irrigation was equal to the amount of rain necessary to prevent negative ASW values (Bryars et al., 2013). The dynamics of the hardwood understory was simulated using the following equations

$$\frac{dWF\_h}{dt} = Bud\_to\_leaf - leaf\_turnover\_h \qquad \text{Equation 40}$$

$$\frac{dWBud\_h}{dt} = NPP\_h \times pF\_h - Bud\_to\_leaf \qquad \text{Equation 41}$$

$$\frac{dWS\_h}{dt} = NPP\_h \times pS\_h - WS_h \times mort\_rate\_h \qquad \text{Equation 42}$$

$$\frac{dWR\_h}{dt} = NPP\_h \times pR\_h - WR_h \times Rttover \qquad \text{Equation 43}$$

$$\frac{dWCR\_h}{dt} = NPP \times pCR\_h - WCR_h \times mort\_rate\_h \qquad \text{Equation 44}$$

Supplemental Table 1. All parameters estimated using data assimilation, prior distributions, and the sensitivity of total biomass at age 25 to the parameter

Parameter	Parameter description	Units	Sensitivity*	Prior distribution	Prior parameters	Reference for prior
pFS2	Ratio of foliage to stem allocation at stem diameter = 2 cm	-	0.00#	Uniform	Min = 1.0 Max = 0.08	Vague
pFS20	Ratio of foliage to stem allocation at stem diameter = 20 cm	-	0.02	Uniform	Min = 1.0 Max =0.1	Vague
pRF	Ratio of fine roots to foliage allocation	-	0.02	Uniform	Min = 0.05 Max = 2	Vague
pCRS	Ratio of coarse roots to stem allocation	-	0.08	Uniform	Min = 0.15 Max = 0.35	1
SLA1	Specific leaf area for mature aged stands	$m^2 kg^{-1}$	0.20	Normal	Mean = 3.58 Sd = 0.11	2
tSLA	Age at which specific leaf area = 1⁄2(SLA0 + SLA1)	Years	0.03	Normal	Mean = 5.97 Sd = 2.15	2
kF	Reduction rate of production per degree Celsius below zero	-	0.00#	Normal	Mean = 0.178 Sd = 0.0162	2
Tmin	Minimum monthly mean temperature for growth	°C	0.02	Normal	Mean = 4 Sd = 2	2,3,4
Topt	Optimum monthly mean temperature for growth	°C	0.28	Normal	Mean = 25 Sd = 2	2,3,4
Tmax	Maximum monthly mean temperature for growth	°C	0.06	Normal	Mean = 38 Sd = 2	2,3,4
MaxAge	Maximum stand age used to compute relative age	Years	0.00#	Uniform	Min = 16 Max = 501	Vague
nAge	Power of relative age in fage	-	0.00#	Uniform	Min = 1 Max = 4	2,3,4
Rttover	Average monthly root turnover rate	$Month^{-1}$	0.01	Uniform	Min = 0.0167 Max = 0.0417	5
MaxCond	Maximum canopy conductance	$m s^{-1}$	0.22	Normal	Mean = 0.0118 Sd = 0.0006	2
LAIgcx	Canopy LAI for maximum canopy conductance	-	0.02	Uniform	Min = 2 Max = 5	2,3,4
CoeffCond	Defines stomatal response to VPD	$mbar^{-1}$	0.22	Normal	Mean = 0.0408 Sd = 0.0028	2
wSx1000	Maximum stem mass per tree at 1000 trees/ha	kg $tree^{-1}$	0.43	Normal	Mean = 235 Sd = 25	2,3,4
thinPower	Power in self thinning law	-	0.25	Uniform	Min = 1.1 Max = 1.80	2,3,4
ms	Fraction of mean stem biomass per tree on dying trees	-	0.15	Uniform	Max = 1 Min = 0.4	Vague

α	Canopy quantum efficiency (pines)	mol C mol PAR^{-1}	0.84	Uniform	Min = 0.02 Max = 0.1	Vague
y	Ratio NPP/GPP	-	0.84	Uniform	Max= 0.66 Min = 0.30	6
fCalpha700	Proportional increase in canopy quantum efficiency between 350 and 700 ppm CO2	-	0.08	Uniform	Min = 1.05 Max = 2.0	Vague
fCpFS700	Proportional decrease in allocation to foliage between 350 and 700 ppm CO2	-	0.00#	Uniform	Min = 0.50 Max = 1.00	Vague
MortRate	Density independent mortality rate (pines)	Month^{-1}	0.02	Uniform	Min = 0.0002 Max = 0.004	Vague
α_h	Canopy quantum efficiency (understory hardwoods)	mol C mol PAR^{-1}	0.00#	Uniform	Min = 0.005 Max = 0.5	Vague
pFS_h	Ratio of foliage to stem partitioning (understory hardwoods)	-	0.00#	Uniform	Min = 0.2 Max = 3.0	Vague
pRF_h	Ratio of foliage to fine roots (understory hardwoods)	-	0.00#	Uniform	Min = 0.05 Max = 2	Vague
SLA_h	Specific leaf area (understory hardwoods)	$m^2 kg^{-1}$	0.00#	Normal	Mean = 16 SD = 3.8	7
SWconst	Moisture ratio deficit when downregulation is 0.5	-	0.06	Uniform	Min = 0.6 Max = 1.8	8, Vague
SWpower	Power of moisture ratio deficit	-	0.06	Uniform	Min = 1 Max= 13	8, Vague
FR1	Fertility rating parameter 1 (mean annual temperature coefficient)	-	0.23	Uniform	Min = 0.0 Max = 1.0	Vague
FR2	Fertility rating parameter 2 (site index age 25 coefficient)	-	0.39	Uniform	Min = 0.0 Max = 1.0	Vague

[1](Albaugh et al., 2005); [2](Gonzalez-Benecke et al., 2016);[3](Bryars et al., 2013);[4](Subedi et al., 2015);[5](Matamala et al., 2003);[6](DeLucia et al., 2007);[7](LeBauer et al., 2010);[8](Landsberg and Waring, 1997), * Sensitivity is 1 when a 10% increase in the parameter results in a 10% change in total biomass. [#]Sensitivity is 0 when a 10% increase in the parameters does not change total biomass by a value greater than 0.01%.

Supplemental Table 2. Parameters not estimated using data assimilation, prior distributions, and the sensitivity of total biomass at age 25 to the parameter

Parameter	Parameter description	Units	Sensitivity	Value	Reference
StemConst	Constant in stem mass vs. diameter relationship	-	0.00	0.1	1
StemPower	Power in stem mass vs. diameter relationship	-	0.01	2.50	1
rAge	Relative age to where fage = 0.5	-	0.00	0.5	2,3,5
BLcond	Canopy boundary layer conductance	$m\ s^{-1}$	0.01	0.1	2,3,5
mF	Fraction of mean foliage biomass per tree on dying trees	-	0.00	0.0	Assumed that all turnover is governed by phenology
mR	Fraction of mean root biomass per tree on dying trees	-	0.00	0.0	Assumed that all turnover is governed by Rttover parameter
fN0	Proportion of LUE at FR = 0	-	0.00	0.0	Set to 0 so that FR represent the proportion of a theoretical maximum
SLA0	Specific leaf area at stand age 0	$m^2\ kg^{-1}$	0.05	5.43	3
k	Extinction coefficient for absorption of PAR by canopy	-	0.28	0.56	2,3,5
fullCanAge	Age at full canopy cover	Years	0.05	3	2,3,5
MaxIntcptn	Maximum proportion of rainfall intercepted by canopy	-	0.03	0.2	2
LAImaxIntcptn	LAI for maximum rainfall interception	-	0.03	5	2
fCg700	Proportional decrease in canopy conductance between 350 and 700 ppm CO2	-	0.01	1	8
pCRS_h	Fraction of stem allocation to coarse roots	-	0.00*	0.2	7
MortRate_h	Density independent mortality rate (understory hardwoods)	$Month^{-1}$	0.00*	0.0009	7

[1](Gonzalez-Benecke et al., 2014a); [2](Bryars et al., 2013); [3](Gonzalez-Benecke et al., 2016); [4](Landsberg and Waring, 1997), [5](Subedi et al., 2015) [6](DeLucia et al., 2007); [7](McCarthy et al., 2010); [8](Ward et al., 2013)

Supplemental Table 3. Posterior means and 95% credible intervals for parameters listed in Table 1 using the data assimilation approaches listed in Table 5.

Parameter	RW	RW-fert	RW-water	DK+NC2	All
pFS2	0.57 (0.54 – 0.61)	0.57 (0.54 – 0.61)	0.60 (0.56 – 0.64)	0.48 (0.42 – 0.57)	0.59 (0.55 – 0.62)
pFS20	0.47 (0.47 – 0.50)	0.52 (0.51 – 0.53)	0.49 (0.48 – 0.50)	0.41 (0.39 – 0.44)	0.51 (0.50 – 0.53)
pRF	0.13 (0.10 – 0.16)	0.17 (0.14 – 0.21)	0.13 (0.10 – 0.16)	0.14 (0.12 – 0.18)	0.12 (0.09 – 0.15)
pCRS	0.26 (0.25 – 0.27)	0.24 (0.23 – 0.25)	0.25 (0.24 – 0.26)	0.17 (0.16 – 0.19)	0.28 (0.27 – 0.29)
SLA1	3.10 (3.01 – 3.18)	3.27 (3.17 – 3.38)	3.12 (3.06 – 3.25)	3.43 (3.31 – 3.53)	3.10 (3.03 – 3.17)
tSLA	5.22 (4.95 – 5.50)	5.52 (5.20 – 5.86)	5.44 (5.16 – 5.76)	8.56 (7.70 – 9.39)	5.32 (4.97 – 5.67)
kF	0.17 (0.14 – 0.20)	0.17 (0.14 – 0.20)	0.17 (0.15 – 0.21)	0.18 (0.14 – 0.21)	0.17 (0.14 – 0.21)
Tmin	-2.44 (-3.44 – -1.27)	-3.11 (-4.85 – -1.80)	-2.09 (-3.00 – -1.12)	-1.40 (-3.00 – -0.01)	-5.47 (-7.57 – -3.54)
Topt	23.72 (22.4 – 25.01)	24.5 (23.0 – 26.0)	24.2 (23.0 – 25.4)	22.5 (21.0 – 24.1)	26.2 (24.2 – 28.2)
Tmax	40.51 (37.3 – 43.75)	39.6 (36.5 – 42.8)	39.7 (36.5 – 43.3)	38.2 (34.5 – 42.0)	40.3 (37.0 – 43.8)
MaxAge	418 (264 – 497)	390 (263 – 495)	407 (268 – 497)	not fit	425 (309 – 498)
nAge	3.54 (2.76 – 3.98)	3.53 (2.71 – 3.98)	3.55 (2.80 – 3.98)	not fit	3.46 (2.63 – 3.98)
Rttover	0.024 (0.018 – 0.029)	0.018 (0.013 – 0.024)	0.027 (0.021 – 0.032)	0.026 (0.020 – 0.033)	0.023 (0.018 – 0.028)
MaxCond	0.011 (0.011 – 0.012)	0.012 (0.011 – 0.012)	0.012 (0.010 – 0.012)	0.011 (0.011 – 0.012)	0.011 (0.010 – 0.012)
LAIgcx	2.31 (2.00 – 2.93)	2.92 (2.73 – 3.00)	2.58 (2.02 – 3.0)	2.05 (2.00 – 2.16)	2.28 (2.02 – 2.77)
CoeffCond	0.037 (0.033 – 0.040)	0.035 (0.031 – 0.039)	0.040 (0.037 – 0.044)	0.040 (0.036 – 0.044)	0.03 (0.029 – 0.038)
wSx1000	176 (171 – 181)	180 (174 – 186)	180 (176 – 186)	258 (228 – 295)	181 (174 0 187)
thinPower	1.67 (1.60 – 1.74)	1.70 (1.63 – 1.78)	1.71 (1.65 – 1.78)	1.28 (1.12 – 1.60)	1.61 (1.51 – 1.69)
ms	0.92 (0.82 – 0.99)	0.98 (0.92 – 1.00)	0.95 (0.85 – 1.00)	0.80 (0.46 – 1.0)	0.83 (0.69 – 0.96)
Alpha	0.037 (0.034 – 0.040)	0.040 (0.036 – 0.045)	0.037 (0.035 – 0.040)	0.035 (0.030 – 0.042)	0.032 (0.030 – 0.035)
y	0.48 (0.46 – 0.51)	0.48 (0.45-0.51)	0.48 (0.46 – 0.51)	0.48 (0.45 – 0.51)	0.52 (0.50 – 0.54)
fCalpha700	1.31 (1.22 – 1.40)	1.31 (1.22 – 1.40)	1.31 (1.22 – 1.40)	1.32 (1.23 – 1.41)	1.11 (1.08 – 1.15)
fCpFS700	0.84 (0.75 – 0.93)	0.83 (0.75 – 0.93)	0.84 (0.75 – 0.93)	0.84 (0.76-0.93)	0.99 (0.95 – 1.0)
MortRate	9.8e-4 (9.2e-4 – 1.0e-3)	1.1e-3 (1.0e-3 – 1.2e-3)	1.0e-3 (1.0e-3 – 1.2e-3)	1.1e-3 (1.0e-3 – 1.2e-3)	1.1e-3 (9.6e-4 – 1.2e-3)
SWconst	1.48 (1.09 – 1.85)	1.31 (0.95 – 1.70)	1.8 (1.47 – 2.15)	1.30 (0.89 – 1.76)	1.57 (1.08 – 1.79)
SWpower	1.61 (0.90 – 2.46)	1.29 (0.78 – 1.98)	2.93 (1.48 – 3.82)	2.20 (1.47 – 3.44)	1.47 (1.09 – 2.26)

FR1	0.094 (0.086 – 0.104)	0.096 (0.088 – 0.103)	0.118 (0.110 – 0.128)	not fit	0.094 (0.087 – 0.102)
FR2	0.144 (0.133 – 0.154)	0.124 (0.108 – 0.142)	0.179 (0.156 – 0.182)	not fit	0.153 (0.140 – 0.168)

Supplemental Table 4. Posterior means and 95% credible intervals for the variance parameters associated with each data stream using the data assimilation approaches listed in Table 5.

Parameter	RW	RW-fert	RW-water	DK+NC2	All
[a]σ_{Stem}	0.13 (0.12 – 0.13)	0.13 (0.12 – 0.13)	0.12 (0.11 – 0.12)	0.06 (0.05-0.07)	0.14 (0.14 – 0.15)
$\sigma_{StemCount}$	106 (104 – 110)	113 (109-116)	111 (108 – 114)	39 (33-47)	137 (131 – 143)
$\sigma_{FineRoots}$	0.76 (0.63 – 0.92)	0.65 (0.48-0.88)	0.83 (0.63 – 1.12)	1.66 (1.23-2.23)	0.83 (0.69 – 1.00)
$\sigma_{CoarseRoots}$	2.3 (1.85 – 2.86)	2.51 (1.98 – 3.05)	2.11 (1.63 – 2.60)	1.87 (1.30 – 2.58)	2.13 (1.62 – 2.68)
σ_{LAI}	0.54 (0.51 – 0.56)	0.52 (0.49 – 0.54)	0.55 (0.53-0.57)	0.56 (0.54-0.58)	0.61 (0.58 – 0.64)
σ_{GEP}	0.78 (0.68)	0.79 (0.69 – 0.89)	0.79 (0.69 – 0.90)	0.79 (0.70 – 0.90)	0.84 (0.74 – 0.96)
σ_{ET}	22.3 (20.0 – 24.7)	22.1 (19.8 – 24.4	22.3 (19.9 – 24.6)	22.3 (20.1 – 24.8)	22.6 (20.1 – 25.7)
$\sigma_{Foliage}$	1.31 (1.23 – 1.39)	1.31 (1.24 – 1.40)	1.43 (1.35 – 1.54)	not fit[b]	1.30 (1.22 – 1.37)
$\sigma_{FoliageProd}$	0.77 (0.66 – 0.90)	0.72 (0.58 – 0.85)	0.78 (0.65 – 0.90)	0.78 (0.65 – 0.91)	1.10 (0.91 – 1.33)
$\sigma_{FineRootProd}$	0.55 (0.46 – 0.65)	0.55 (0.43 – 0.66)	0.55 (0.45 – 0.65)	0.55 (0.44 – 0.67)	0.83 (0.69 – 1.00)

[a]standard deviation is proportion to the stem biomass; [b]foliage biomass observations were not used in the DK+NC2 simulations because LAI and foliage production observations were available.

Supplemental Figures

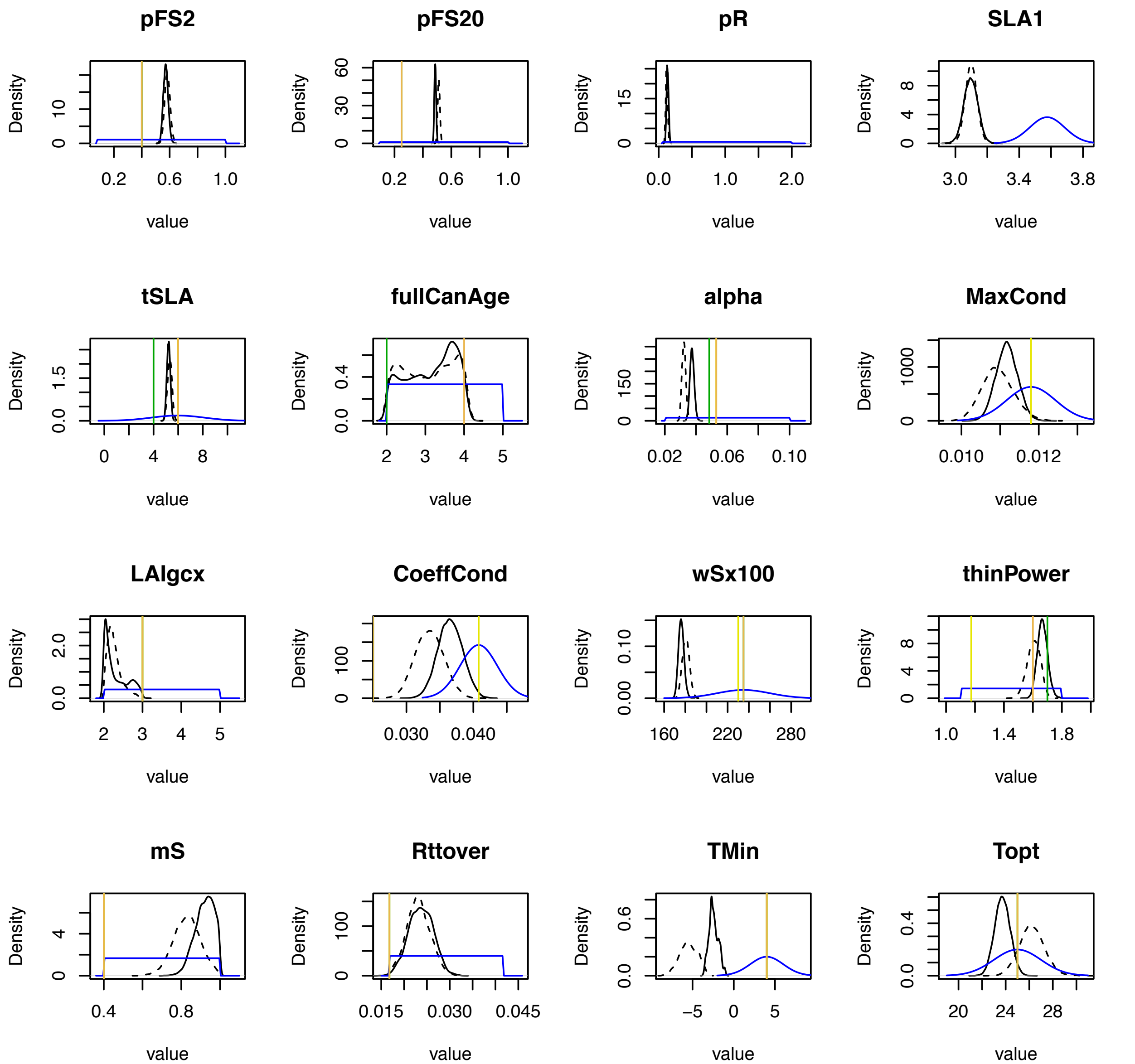

Supplemental Figure 1. Prior (blue line), posterior (black lines) and parameter values used in previous applications of the 3-PG model (yellow, green, and tan lines) for the parameters in Table 1. The posteriors for the 1-stage (dashed black line) and 2-stage (solid black line) data assimilation approaches are shown. See Supplement Figure 3 for the legend.

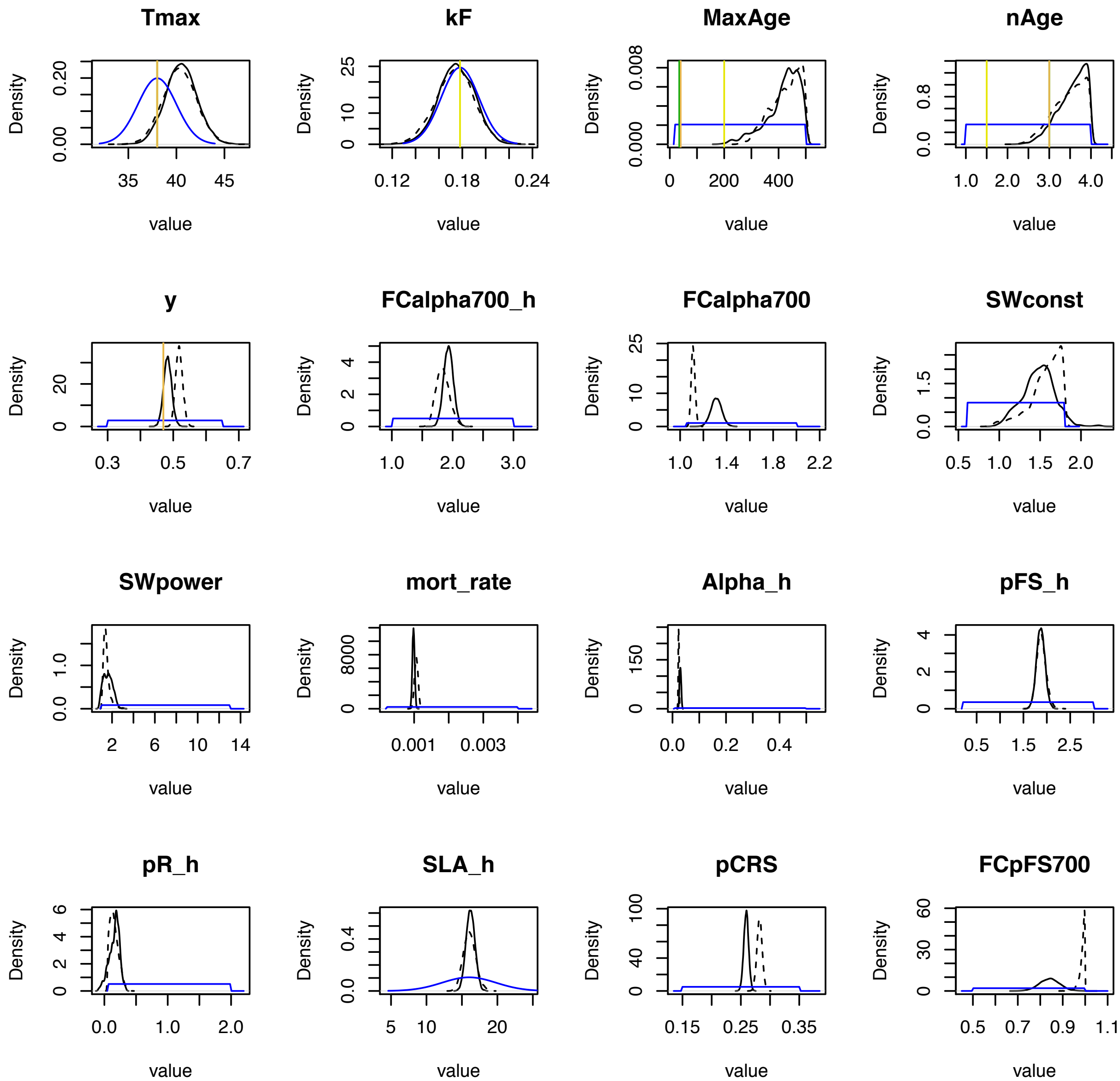

Supplemental Figure 2. Continued from Supplemental Figure 1

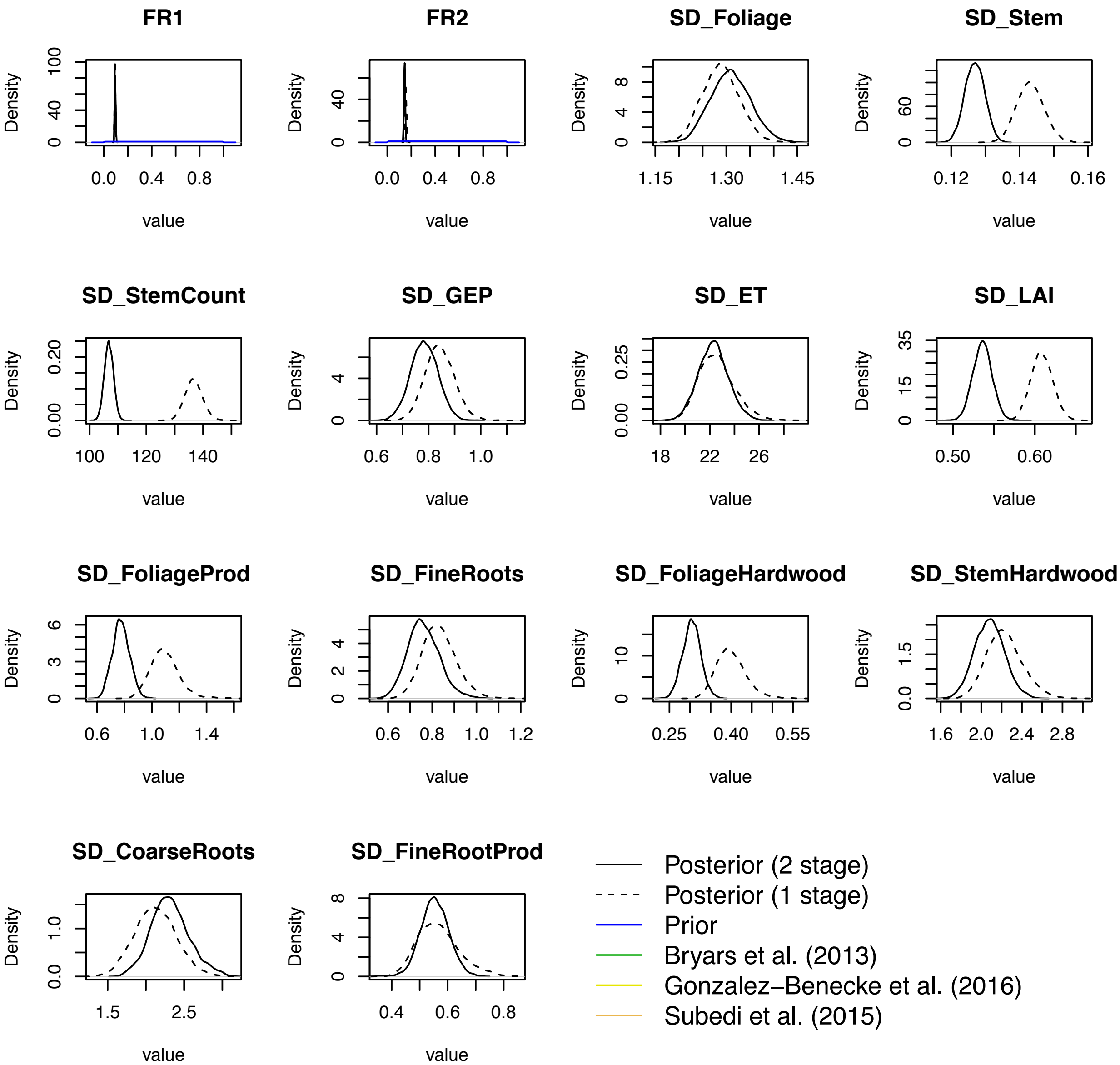

Supplemental Figure 3. Continued from Supplemental Figure 2.

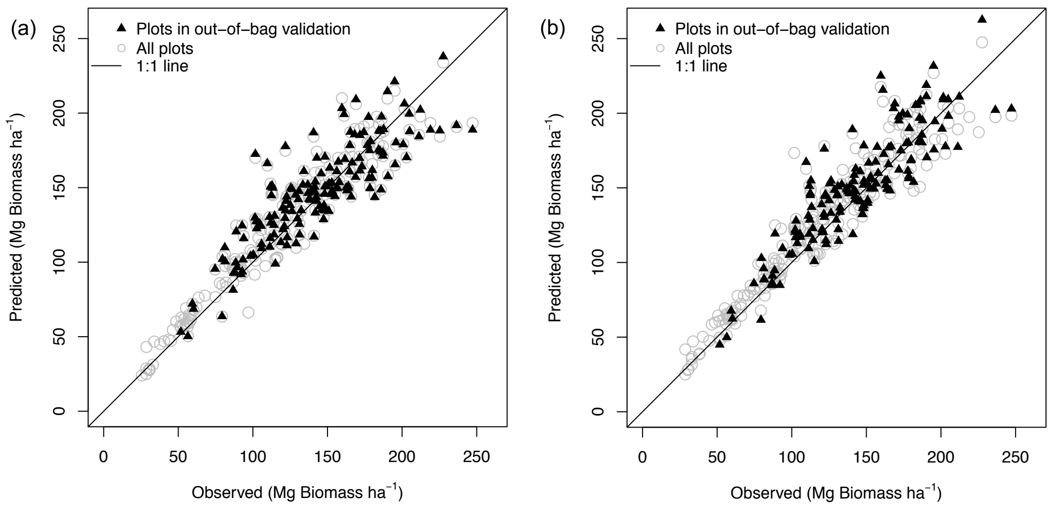

Supplemental Information Figure 1. Model evaluation of stem biomass using the (a) RW-fert and (b) RW-water data assimilation approaches described in Table 5. The gray circles correspond to predictions where all plots were used in data assimilation. The black triangles correspond to predictions where 120 plots were not included in data assimilation and represent an independent evaluation of model predictions (out-of-bag validation). For each plot, we used the measurement with the longest interval between initialization and measurement for evaluation.

References

Abatzoglou, J. T.: Development of gridded surface meteorological data for ecological applications and modelling, International Journal of Climatology, 33(1), 121–131, doi:10.1002/joc.3413, 2013.

Albaugh, T. J., Allen, H. L. and Kress, L. W.: Root and stem partitioning of *Pinus taeda*, Trees, 20(2), 176–185, doi:10.1007/s00468-005-0024-4, 2005.

Albaugh, T. J., Allen, H. L., Stape, J. L., Fox, T. R., Rubilar, R. A., Carlson, C. A. and Pezzutti, R.: Leaf area duration in natural range and exotic *Pinus taeda*, Can. J. For. Res., 40(2), 224–234, doi:10.1139/X09-190, 2010.

Almeida, A. C., Sands, P. J., Bruce, J., Siggins, A. W., Leriche, A., Battaglia, M. and Batista, T. R.: Use of a spatial process-based model to quantify forest plantation productivity and water use efficiency under climate change scenarios, pp. 1816–1822, Cairns. 2009.

Bryars, C., Maier, C., Zhao, D., Kane, M., Borders, B., Will, R. and Teskey, R.: Fixed physiological parameters in the 3-PG model produced accurate estimates of loblolly pine growth on sites in different geographic regions, Forest Ecol Manag, 289, 501–514, doi:10.1016/j.foreco.2012.09.031, 2013.

DeLucia, E. H., Drake, J. E., Thomas, R. B. and Gonzalez-Meler, M.: Forest carbon use efficiency: is respiration a constant fraction of gross primary production? Global Change Biology, 13(6), 1157–1167, doi:10.1111/j.1365-2486.2007.01365.x, 2007.

Gonzalez-Benecke, C. A., Gezan, S. A., Albaugh, T. J., Allen, H. L., Burkhart, H. E., Fox, T. R., Jokela, E. J., Maier, C. A., Martin, T. A., Rubilar, R. A. and Samuelson, L. J.: Local and general above-stump biomass functions for loblolly pine and slash pine trees, Forest Ecol Manag, 334, 254–276, doi:10.1016/j.foreco.2014.09.002, 2014a.

Gonzalez-Benecke, C. A., Jokela, E. J., Cropper, W. P., Jr, Bracho, R. and Leduc, D. J.: Parameterization of the 3-PG model for Pinus elliottii stands using alternative methods to estimate fertility rating, biomass partitioning and canopy closure, Forest Ecol Manag, 327(C), 55–75, doi:10.1016/j.foreco.2014.04.030, 2014b.

Gonzalez-Benecke, C. A., Teskey, R. O., Martin, T. A., Jokela, E. J., Fox, T. R., Kane, M. B. and Noormets, A.: Regional validation and improved parameterization of the 3-PG model for Pinus taeda stands, Forest Ecol Manag, 361, 237–256, doi:10.1016/j.foreco.2015.11.025, 2016.

Landsberg, J. and Waring, R.: A generalised model of forest productivity using simplified concepts of radiation-use efficiency, carbon balance and partitioning, Forest Ecol Manag, 95(3), 209–228, doi:10.1016/S0378-1127(97)00026-1, 1997.

LeBauer, D. S., Dietze, M., Long, S., Mulrooney, P., Rohde, G. S., Wang, D. and Kooper, R.: *Biofuel Ecophysiological Traits and Yields Database (BETYdb)*,, doi:doi:10.13012/J8H41PB9, 2010.

Matamala, R., Gonzàlez-Meler, M. A., Jastrow, J. D., Norby, R. J. and Schlesinger, W. H.: Impacts of fine root turnover on forest NPP and soil C sequestration potential, Science, 302(5649), 1385–1387, doi:10.1126/science.1089543, 2003.

McCarthy, H. R., Oren, R., Johnsen, K. H., Gallet-Budynek, A., Pritchard, S. G., Cook, C. W., LaDeau, S. L., Jackson, R. B. and Finzi, A. C.: Re-assessment of plant carbon dynamics at the Duke free-air CO2 enrichment site: interactions of atmospheric [CO2] with nitrogen and water availability over stand development, New Phytol, 185(2), 514–528, doi:10.1111/j.1469-8137.2009.03078.x, 2010.

Sabatia, C. O. and Burkhart, H. E.: Predicting site index of plantation loblolly pine from biophysical variables, Forest Ecol Manag, 326, 142–156, doi:10.1016/j.foreco.2014.04.019, 2014.

Sampson, D. A., Albaugh, T. J., Johnsen, K. H., Allen, H. L. and Zarnoch, S. J.: Monthly leaf area index estimates from point-in-time measurements and needle phenology for Pinus taeda, Can. J. For. Res., 33(12), 2477–2490, doi:10.1139/x03-166, 2003.

Subedi, S., Fox, T. and Wynne, R.: Determination of fertility rating (FR) in the 3-PG model for loblolly pine plantations in the Southeastern United States based on site index, Forests, 6(9), 3002–3027, doi:10.3390/f6093002, 2015.

Ward, E. J., Oren, R., Bell, D. M., Clark, J. S., McCarthy, H. R., Kim, H.-S. and Domec, J.-C.: The effects of elevated CO_2 and nitrogen fertilization on stomatal conductance estimated from 11 years of scaled sap flux measurements at Duke FACE, Tree Physiology, 33(2), 135–151, doi:10.1093/treephys/tps118, 2013.